

# Distinctions Between Islet and Acinar Cells in Mammalian Pancreatic Tissue Using High Field MR Microscopy

S. C. Grant<sup>1,2</sup>, N. E. Simpson<sup>3</sup>, S. A. Litherland<sup>4</sup>, S. J. Blackband<sup>2,5</sup>, I. Constantinidis<sup>3</sup>

<sup>1</sup>Chemical and Biomedical Engineering, Florida State University, Tallahassee, FL, United States, <sup>2</sup>National High Magnetic Field Laboratory, Tallahassee, FL, United States, <sup>3</sup>Medicine, Division of Endocrinology, University of Florida, Gainesville, FL, United States, <sup>4</sup>Pathology, Immunology, and Laboratory Medicine, University of Florida, Gainesville, FL, United States, <sup>5</sup>Neuroscience, University of Florida, Gainesville, FL, United States

**Introduction** Diabetes Mellitus is inextricably linked to the loss of functionality in the insulin-producing islets cells of the endocrine pancreas. However, because they are less than 400- $\mu\text{m}$  in size and constitute less than 2% of the adult pancreas, islet cells have been traditionally difficult to image *in vivo* and yield relatively few specimens per procedure for *ex vivo* research. Recently, a limited number of studies have attempted to image excised mammalian pancreatic tissue in efforts to understand autoimmune response destruction via labeled lymphocytes (1), to investigate encapsulation techniques for islet implantation (2,3) and to interrogate isolated islet organization in hopes of elucidating a morphometric link between structure and viability (4). The current study builds upon these earlier efforts to examine native differences in organization between viable, isolated islet cells and the acinar cells that surround and support them. Using high field MR microscopy conducted at 17.6 T, porcine and human samples of isolated islet and acinar cells display distinctly unique cellular organizations that are corroborated by optical images obtained with deconvolution confocal microscopy. Further, quantification of MR parameters in isolated islet and acinar cells belies differences in the heterogeneity of these samples.

**Methods** Porcine pancreatic islets were processed independently and harvested at the University of Minnesota. Islets were made available for this study within 24 hrs of isolation. Prior to imaging, islets were maintained in fresh medium consisting of CMRL supplemented with 15% horse serum, 2.5% bovine serum, 1% penicillin-streptomycin and L-glutamine to a final concentration of 6 mM. All porcine preparations were >90% pure and >90% viable. An aliquot from every shipment was stained with dithizone upon their arrival to test rudimentary insulin secreting ability and were examined within 24 hrs. For comparison, multicellular aggregates (>100- $\mu\text{m}$  diameters) of murine insulinomas  $\beta\text{TC3}$  cells also were examined. All samples were imaged without encapsulation, freely floating in the appropriate media.

**MR imaging:** MRI data were acquired using a vertical widebore 17.6-T magnet equipped with a Bruker Avance console and Micro2.5 gradients. Samples were loaded into a capillary with an outer/inner diameter of 700/530  $\mu\text{m}$ . The capillary was placed within a homebuilt solenoidal microcoil measuring 850  $\mu\text{m}$  in diameter. Control experiments determined that this practice was not detrimental to the islets over the imaging period. A series of high resolution images was obtained using spin echo (SE) and gradient echo (GE) sequences to develop diffusion-, T<sub>2</sub>- and T<sub>2</sub>\*-weighted contrast. A modified multi-slice SE sequence with balanced bipolar gradients was used to acquire microimages with and without diffusion weighting (b value = 1000 s/mm<sup>2</sup>). With a total acquisition time of approximately 1.1 hours, these images were acquired at an in-plane resolution of at least 25 x 25  $\mu\text{m}$  and slice thickness of 200  $\mu\text{m}$  with a repetition time (TR) of 2000 ms. To quantify T<sub>2</sub>, the SE sequence was acquired at multiple echo times (TE). 3D GE images were acquired using a TE/TR of 15/150 ms within 2.75 hrs at an isotropic resolution of at least 15  $\mu\text{m}$ . 3D GE acquisitions also were acquired at lower resolutions with TE incremented from 4 to 25 ms to sample T<sub>2</sub>\*. All quantitative data was fit to a single decaying exponential.

**Confocal microscopy:** Live islets, acinar cells and  $\beta\text{TC3}$  aggregates were placed in coverslip bottom dishes and stained with SYTO 41 (blue, Molecular Probes, Invitrogen), a fluorescent vital cell-permeable nucleic acid dye that stains the nucleus of eukaryotic cells. Immunofluorescence images were collected using a Delta Vision Deconvolution microscopy system with an Olympus OMT inverted microscope at room temperature. Images were processed with 15 reiterations of the deconvolution algorithm and visualized as individual optical slices (0.5-1  $\mu\text{m}$  thick) or 3D reconstructions of twenty such slices. 3D images were analyzed in 360° rotations to visualize the nuclear and cytoplasmic portions of the cells in 2 separate planes and to detect the relative 3D position of cells relative to each other.

## Results and Discussion

As shown in Fig. 1, T<sub>2</sub>- and diffusion-weighted images with corresponding optical deconvolution confocal microscopy (ODCM) present striking differences between of porcine islets and  $\beta\text{TC3}$  aggregates. The multicellular aggregates display a compact and uniform spheroid of cells that appears generally homogenous for the 3 imaging techniques presented while isolated islets demonstrate a marked heterogeneity in both MR and ODCM images. Quantification of MR coefficients also supports this heterogeneity, with the higher ADC and T<sub>2</sub> values of isolated islets indicating a looser organization. This heterogeneous organization is pointedly evident in the high resolution images of Fig 2. As with the ODCM images, there is continuity between adjacent MR slices that betrays an ordering of cells (and possibly intracellular regions) throughout the isolated islet. Fig 3. displays the readily apparent differences in image contrast between islets and adjacent acinar cells in a cluster of pancreatic tissue. This heterogeneity and gross viability was confirmed by dithizone staining (Fig. 3B). Additionally, Figs 3C&D provide evidence from immunofluorescence ODCM staining that corroborates the MR images. Acinar cells display fairly uniform distributions of cytoplasm and nuclear regions while isolated islets appear much less homogenous with regard to these two subcellular structures.

In summary, MR microimages demonstrate that isolated islets possess a structural heterogeneity previously unseen. A clear distinction between islets and surrounding acinar tissue based on the unique heterogeneity of islet has been reported for the first time. Furthermore, optical images obtained with deconvolution confocal microscopy support the MR observations of an intra-islet structural organization.

**Acknowledgments and References** Financial support provide by the NIH (R01 DK56890, R01 DK47858 and P41 RR16105) and the NSF through the National High Magnetic Field Laboratory. MRI data were obtained at the Advanced Magnetic Resonance Imaging and Spectroscopy (AMRIS) facility in the McKnight Brain Institute of the University of Florida. We also would like to thank Drs. Bernhard Hering and Klearchos Pappas of the University of Minnesota for facilitating the procurement of porcine islets.

- (1) Moore, A. et al. MRI of insulinitis in autoimmune diabetes. *Magnetic Resonance in Medicine* 47, 751-758 (2002).
- (2) Constantinidis, I., et al., A. Non-invasive monitoring of a bioartificial pancreas in vitro and in vivo. *Annals New York Academy Sciences* 944, 83-96 (2001).
- (3) Gimi, B. et al. NMR Spiral Surface Microcoils: Applications. *Concepts Magnetic Resonance Part B (Magn Reson Engineering)* 18B, 1-8 (2003).
- (4) S.C.Grant, et al., MR Microscopy of Pancreatic Islets of Langerhans. *ISMRM: 12th Scientific Meeting and Exhibition*, 358, (2004).

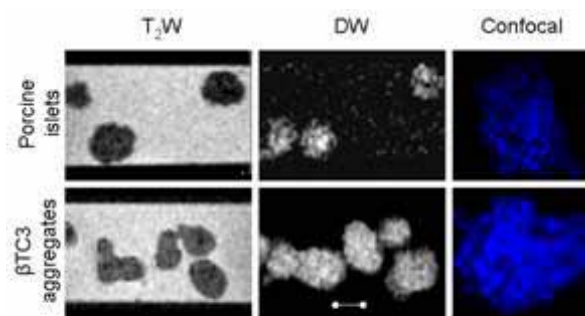


**FIGURE 1:** T<sub>2</sub> and diffusion weighted MR images and deconvolution 3D images of porcine islets and  $\beta\text{TC3}$  multicellular aggregates. The reference bar in the MR images represents 100  $\mu\text{m}$ . Confocal images are reconstructed from 20 Z-axis slices at 0.5- $\mu\text{m}$  thickness.

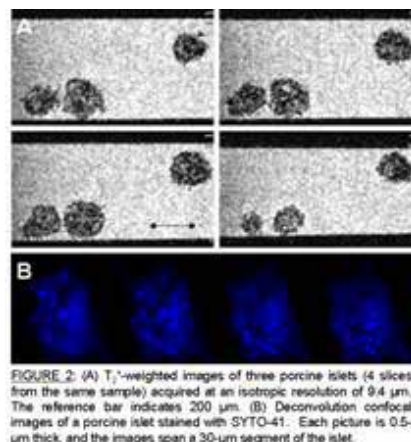


**FIGURE 2:** (A) T<sub>1</sub>-weighted images of three porcine islets (4 slices from the same sample) acquired at an isotropic resolution of 9.4  $\mu\text{m}$ . The reference bar indicates 200  $\mu\text{m}$ . (B) Deconvolution confocal images of a porcine islet stained with SYTO-41. Each picture is 0.5- $\mu\text{m}$  thick, and the images span a 30- $\mu\text{m}$  segment of the islet.

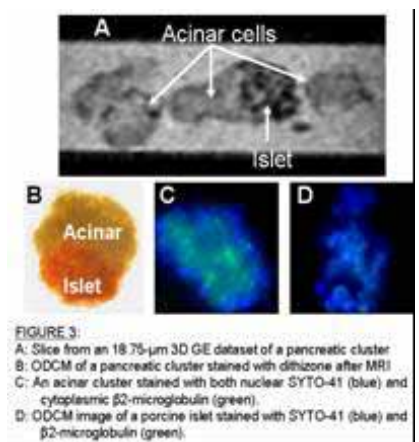


**FIGURE 3:** A: Slice from an 18.75- $\mu\text{m}$  3D GE dataset of a pancreatic cluster B: ODCM of a pancreatic cluster stained with dithizone after MRI C: An acinar cluster stained with both nuclear SYTO-41 (blue) and cytoplasmic  $\beta\text{2}$ -microglobulin (green). D: ODCM image of a porcine islet stained with SYTO-41 (blue) and  $\beta\text{2}$ -microglobulin (green).